Comparative Studies on Isomerization Behavior and Photocontrol of Nematic Liquid Crystals Using Polymethacrylates with 3,3′- and 4,4′-Dihexyloxyazobenzenes in Side Chains

Christian Ruslim and Kunihiro Ichimura*

Research Laboratory of Resources Utilization, Tokyo Institute of Technology, 4259 Nagatsuta, Midori-ku, Yokohama 226-8503, Japan

Received January 25, 1999; Revised Manuscript Received April 6, 1999

ABSTRACT: Azobenzene moieties with 3,3′-dihexyloxy-2,2′-dimethyl and 4,4′-dihexyloxy substituents were attached to backbones of polymethacrylates at low contents (7 mol %) to investigate the effect of positional isomerism of the substituents on photochemical and thermal isomerization behavior and the ability to perform the surface-assisted alignment control of liquid crystals photochemically. Photoisomerization in thin films in a glassy state through $\pi-\pi^*$ excitation deviates markedly from those in solutions, but that through $n-\pi^*$ excitation takes the behavior of solution photoisomerization. This can be explained in terms of the difference in sweep volumes (critical volumes needed for isomerization) of the azobenzenes in relation to the mechanisms of the isomerization. Polarized light-induced anisotropy of the polymer thin films gave rise to the photocontrollability of alignment of a nematic liquid crystal, despite low azo-chromophore contents. Photoorientation and photoreorientation of the nematic liquid crystal depend significantly on sweep volumes for the photoisomerization which is controlled by the selection of the excitation wavelength and the molecular conformation of the azo-chromophores.

Introduction

The incorporation of photoisomerizable azobenzene molecules in polymer matrixes has been the trend of current research in the area of optical devices because of the mutual exploitable characteristic performances, that is the ease of device fabrication and the photoresponsiveness of azobenzene units, which can trigger property changes as a result of the conformational change of the molecules.[1] However, this tremendous practical research involving the photoisomerization of azobenzenes lacks a comprehensive explanation of the nature of the isomerization processes in relation to their molecular structures. As has been recognized for a long time, isomerization behavior in polymer matrixes differs from that in solution and involves fast and slow processes because of the restricted mobility in the vicinity of the free volume. Isomerization of azobenzenes in polymer matrixes has been used to probe the distribution of free volume of the polymers[2−5] and to study mechanisms of photoisomerization and thermal relaxation of the chromophore itself.[6−11]

On probing the distribution of free volume of glassy polymers, an implicit assumption is usually made that the probe azobenzene represents the average free volume environment. In this context, the existence of the two isomerization mechanisms, rotation and inversion, should also be taken into consideration. Some experimental and theoretical evidence supports that isomerization through $\pi-\pi^*$ excitation of azobenzene proceeds with the rotation mechanism, whereas $n-\pi^*$ excitation proceeds purely with inversion.[12−15] A restricted environment can influence the mechanism of isomerization.

In the case of thermal *Z*-to-*E* isomerization, Paik and Morawetz interpreted the anomalously fast reaction in polymer matrixes at the early stage in terms of the relaxation of the *Z*-isomers in a strained conformation.[8] On the other hand, Eisenbach correlated this phenomenon to the occurrence of the translational relaxation of local polymer segments, whereas the normal reaction is attributed to the rotational relaxation of the neighboring polymer segments associated with the local distribution of free volume.[9,10]

Since we have been systematically dealing with "command surfaces", the photocontrol of the molecular orientation of liquid crystal (LC) alignment using surface-modified photosensitive molecules, in this case, azobenzenes, is of great importance to explore in detail the effect of conformational structures and isomerization mechanisms on the performance of the aligning layers.[16,17] In this paper, we propose a novel azobenzene chromophore having 3- and 3′-substituents to investigate its isomerization characteristics in comparison with those of a chromophore having 4- and 4′-substituents and with those of the azobenzenes in the literature. The importance of exploiting the properties of 3,3′-disubstituted azobenzene is attributed to the following. (1) Recently, we have reported that when selective elongated substituents embed in the 3- and 3′-positions of an azobenzene, the molecule may have a rodlike *Z*-isomer compatible with LC molecules, as has also been predicted by the molecular calculation for the stable conformation at the ground state.[18,19] This kind of azobenzene derivative has a smaller sweep volume for isomerization in comparison to those of the analogous 4,4′-substituted azobenzenes. (2) Information on properties of azobenzene molecules with *meta*-substituents has been insufficient. We assume that the comparison of their properties to those of the intensively studied *para*- or *ortho*-substituted azobenzenes will also be feedback regarding already known characteristics. (3) In the context of our systematic research on "command surfaces" incorporating azobenzene molecules, the employment of *E*/*Z* azobenzene isomers exhibiting marked

* To whom correspondence should be addressed. Telephone: +81-45-924-5266. Fax: +81-45-924-5276. E-mail: kichimur@res.titech.ac.jp.

10.1021/ma990102d CCC: $18.00
Published on Web 06/11/1999

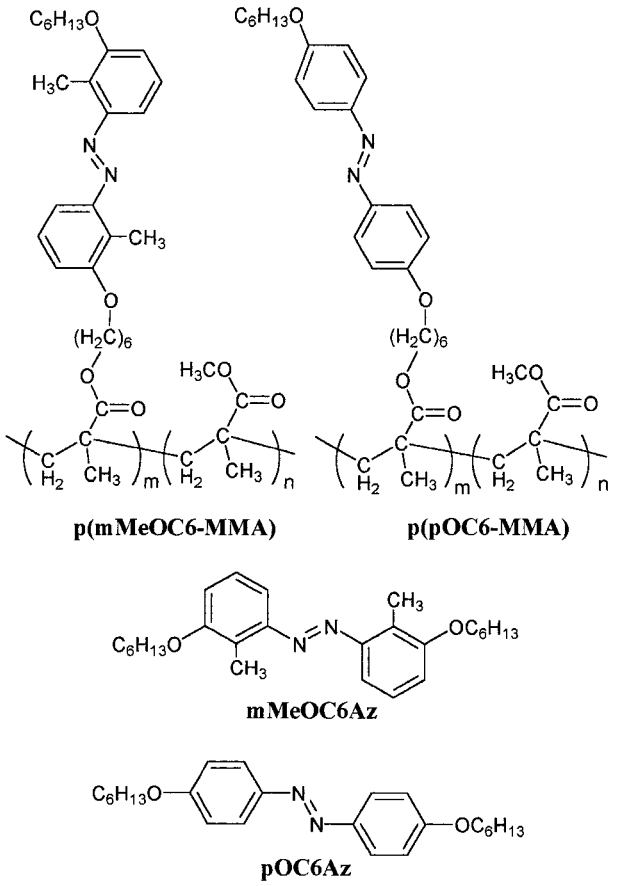

Figure 1. Structures of azobenzene polymers and low-mass azobenzenes.

differences in the conformation in polymeric systems is a novel approach for revealing the relation between isomerization behavior and LC photocontrol.

We present here the first preparation of polymethacrylates with 3,3′-substituted azobenzenes as side chains. The photoisomerization by UV and visible light excitation is investigated and compared to that of a 4,4′-disubstituted azobenzene. Thermal *Z*-to-*E* relaxation of the polymers will also be discussed. Essentially, the ability of the polymers as LC photoalignment layers using linearly polarized light is examined, focusing on the effect of isomerization behavior on the performance of photoorientation and photoreorientation of nematic LCs.

Experimental Section

Materials. Hexyl bromide and methyl methacrylate were purchased from Tokyo Kasei Kogyo Co., Ltd. Methyl methacrylate was distilled under reduced pressure before used. 6-Bromohexanol, 4-hexyloxyaniline, and PMMA (T_g = 114 °C) from Aldrich, methacryloyl chloride and AIBN from Kanto Chemicals, and phenol from Wako Pure Chemicals were used as received. DMF was distilled from molecular sieves, and THF, from $LiAlH_4$. Preparations of **pOC6Az** and **mMeOC6Az** (see Figure 1) for dispersed systems and 3,3′-dihydroxy-2,2′-dimethylazobenzene have been previously reported.[19]

2,2′-Dimethyl-3-hydroxy-3′-hexyloxyazobezene. In a 20 mL DMF solution was dissolved 3,3-dihydroxy-2,2′-dimethylazobenzene (1.00 g; 4.1 mmol), potassium carbonate (1.43 g; 10.4 mmol), and a small amount of potassium iodide. The mixture was stirred and heated at 70 °C for 30 min before hexyl bromide (0.81 g; 4.9 mmol) was added dropwise. The end of the reaction was determined by TLC, and the product was purified by column chromatography on silica gel using a 5:1 mixture of hexane and ethyl acetate as an eluent. A 42% yield of orange product (mp 95−97 °C) was obtained. ^{1}H NMR (200 MHz, $CDCl_3$) δ 0.92 (t, J = 6.8 Hz, 3H), 1.33−1.58 (m, 6H), 1.86 (quintet, J = 6.5 Hz, 2H), 2.62 (s, 3H), 2.64 (s, 3H), 4.03 (t, J = 6.4 Hz, 2H), 6.88−7.28 (m, 6H).

2,2′-Dimethyl-3-hexyloxy-3′-(6-hydroxy)hexyloxyazobenzene. This was prepared from 2,2′-dimethyl-3-hexyloxy-3′-hydroxyazobenzene (0.46 g; 1.41 mmol) and 6-bromohexanol (0.29 g; 1.60 mmol) by the same method as described above in 95% yield (mp 91−93 °C). ^{1}H NMR (200 MHz, CDCl) δ 0.92 (t, J = 6.8, 3H), 1.19−1.67 (m, 13H), 1.84 (quintet, J = 6.5 Hz, 4H), 2.61 (s, 6H), 3.67 (m, 2H), 4.03 (t, J = 6.4 Hz, 4H), 6.89−7.26 (m, 6H).

4-Hydroxy-4′-hexyloxyazobenzene. This was prepared from 4-hexyloxyaniline (3.00 g; 15.5 mmol) and phenol (1.50 g; 15.5 mmol) by the azo-coupling method. The product was purified by flash column chromatography and recrystallization from ethyl acetate to give a brown solid (mp 97−99 °C) in 29% yield. ^{1}H NMR (200 MHz, $CDCl_3$) δ 0.91 (t, J = 6.7 Hz, 3H), 1.31−1.55 (m, 6H), 1.82 (quintet, J = 6.3 Hz, 2H), 4.03 (t, J = 6.5 Hz, 2H), 5.05 (s, 1H), 6.90−7.01 (m, 4H), 7.81−7.88 (m, 4H).

4-Hexyloxy-4′-(6-hydroxy)hexyloxyazobenzene. This was prepared in a similar way as that for 2,2′-dimethyl-3-hexyloxy-3′-(6-hydroxy)hexyloxyazobenzene. Recrystallization from acetone provided a yellow solid (crystalline 115 °C LC 119 °C isotropic) in 83% yield. ^{1}H NMR (200 MHz, $CDCl_3$) δ 0.89 (t, J = 6.9 Hz, 3H), 1.35−1.88 (m, 16H), 3.67 (m, 2H), 4.03 (t, J = 6.4 Hz, 4H), 6.98 (d, J = 8.6 Hz, 4H), 7.86 (d, J = 9.2 Hz, 4H).

Monomer Synthesis. 2,2′-Dimethyl-3-(6-methacryloylhexyloxy)-3′-hexyloxyazobenzene. A mixture of 2,2′-dimethyl-3-hexyloxy-3′-(6-hydroxy)hexyloxyazobenzene (0.57 g; 1.34 mmol), triethylamine (0.4 g; 3.95 mmol), and methacryloyl chloride (0.25 g; 2.39 mmol) in 30 mL of THF was stirred for 30 min at 0 °C and then at room temperature for 2 h. The product was purified by flash chromatography and recrystallization from a THF/hexane solution to give an orange product (crystalline 54 °C LC 65 °C isotropic) in 58% yield. ^{1}H NMR (200 MHz, $CDCl_3$) δ 0.89 (t, J = 6.9 Hz, 3H), 1.34−1.95 (m, 19H), 2.61 (s, 6H), 4.03 (t, J = 6.5 Hz, 4H), 4.18 (t, J = 6.6 Hz, 2H), 5.54 (t, J = 1.5 Hz, 1H), 6.10 (s, 1H), 6.89−7.28 (m, 6H). Calcd. for $C_{30}H_{42}N_2O_4$: C, 72.83; H, 8.57; N, 5.66. Found: C, 7.55; H, 8.53; N, 5.33.

4-(6-Methacryloylhexyloxy)-4′-hexyloxyazobenzene. This was prepared in the same manner as that for the above monomer from 4-hexyloxy-4′-(6-hydroxy)hexyloxyazobenzene (0.48 g; 1.20 mmol) and methacryloyl chloride (0.16 g; 1.53 mmol). A yellow product (crystalline 77 °C LC 85 °C isotropic) was obtained in 68% yield. ^{1}H NMR (200 MHz, $CDCl_3$) δ 0.92 (t, J = 6.8 Hz, 3H), 1.35−1.95 (m, 19H), 4.01 (t, J = 6.5 Hz, 4H), 4.17 (t, J = 6.5 Hz, 2H), 5.54 (t, J = 1.6 Hz, 1H), 6.10 (s, 1H), 6.99 (d, J = 9.0 Hz, 4H), 7.85 (d, J = 9.0 Hz, 4H). Calcd. for $C_{28}H_{38}N_2O_4$: C, 72.06; H, 8.22; N, 6.00. Found: C, 7.33; H, 8.09; N, 5.76.

Polymerization. A degassed THF solution of a 25 wt % azobenzene monomer with methyl methacrylate (azobenzene/methyl methacrylate = 1:10) and 0.50 wt % AIBN in an ampule was shaked at 65 °C for 12 h. Precipitation of a polymeric product in methanol was repeated twice. The polymer was finally dried in a vacuum at room temperature.

Physical Measurements. The chemical structures of products were characterized by ^{1}H NMR spectra, recorded on a Bruker AC-200 NMR spectrometer with TMS as an internal standard, and elemental analysis. Phase transition points were determined with a micromelting apparatus (Yanaco MP-S3) and a polarized optical microscope (Olympus BH-2) equipped with a hot stage (Mettler FP800). The glass transition temperatures of the copolymers were measured with a DSC 22C (Seiko Electronics). Copolymerization ratios were estimated from ^{1}H NMR spectra. Molecular weight was determined by gel permeation chromatography (JASCO) at a flow rate of 1.0 mL/min with THF as the eluent, on the basis of the molecular weight of a standard polystyrene calibration curve.

Table 1. Properties of Polymethacrylates with Azobenzene Moieties in Side Chains

polymer	azo-monomer/MMA ratio feed	azo-monomer/MMA ratio result	mol. wt $10^{-4}M_w$	mol. wt M_w/M_n	yield (%)	T_g [°C]
p(mMeOC6-MMA)	1:10	1:13	6.5	2.8	77	93
p(pOC6-MMA)	1:10	1:13	6.5	2.7	81	96

UV/vis spectra were recorded on a diode array spectrometer (HP8452A). Photoisomerization was carried out by using 365 and 436 nm light from a Hg−Xe lamp (San-Ei Supercure-203S) passing through UV35/UVD36 and Y43/V44 glass filters (Toshiba), respectively, with or without a polarizer (Glan-Thomson). Light intensity was measured with an optical power meter (Advantest TQ8210). A hot stage (Mettler FP800) was used to control the temperatures of samples for thermal *Z*-to-*E* relaxation experiments.

Sample Preparation. Photochemical and thermal reactions of the copolymers were investigated in solutions and in spin-cast thin films. Solution reaction was carried out by irradiating a THF solution of a polymer with azobenzene side chains (ca. 10^{-5} mol dm^{-3}) in a 1 cm thick quartz cell with UV or visible light. In the case of a solid-state reaction, a 3 wt % polymer solution in toluene was adjusted, spin-coated on a cleaned quartz plate, and dried in an oven at 100 °C for 2 h to obtain thin films of 90−100 nm thickness. In a dispersed system, the concentrations of low-molecular-weight azobenzene in PMMA were made on the order of 10^{-3} mol dm^{-1} by mixing a 20 wt % PMMA solution and a 0.2 wt % solution of the low-mass azobenzene in toluene at a ratio of four to one. Within this concentration range, no aggregation of azo-chromophores occurs.[20] Cast films were allowed to dry slowly in a capped Petri dish at room temperature overnight before being subjected to a vacuum oven at 120 °C for 2 h to get films about 20−40 μm thick.

Hybrid LC cells were fabricated by using a spin-coated polymer and lecithin-treated plates between which a nematic LC was injected above its T_{NI}. The cell gap was controlled using silica spacers 5 μm in diameter. To evaluate the photoalignment of an LC, a probing He−Ne laser beam was passed through the LC cell and a polarizer to measure the transmittance as a function of rotational angle of the cell.

Results and Discussion

Molecular Design. The chemical structures of polymers and low-mass azobenzenes are shown in Figure 1. Elongated substituents are incorporated with the following anticipation. (1) Substituents at both ends of azobenzenes should give a rather clear difference distinguishing the effect of positional isomerism on an average sweep volume between the two azobenzenes. (2) The interplay between the chromophore and the nematic LC to be aligned can be enhanced through alkyl chain interactions.

Aggregation of azobenzene chromophores in the polymeric systems has an extreme effect on isomerization behaviors as well as on the orientation of the chromophores.[21−23] By making the content of azobenzene low enough, we can ignore such an effect, giving us more ease in analyzing only the monomeric characteristics in photoalignment. Copolymerization results are listed in Table 1. The content of azo-chromophores was approximately 7 mol %. The fact that the degree of polymerization, the molecular weight, and T_g are very similar gives us great convenience in comparing their properties, since the dependence of these quantities can be suppressed.

Photoisomerization Characteristics. The λ_{max} values of the polymer thin films are the same as those in THF, that is at 330 nm for **p(mMeOC6-MMA)** and 360 nm for **p(pOC6-MMA)**. The low-mass azobenzenes (**mMeOC6Az** and **pOC6Az**) dispersed in PMMA in a dilute concentration also exhibited the same λ_{max}. Examples of the spectral changes during irradiation with 365 nm light and 436 nm light are shown in Figures 2 and 3, respectively. Upon photoisomerization, isosbestic points at 237, 256, 285, and 404 nm for **p(mMeOC6-MMA)** and at 242, 252, 320, and 428 nm for **p(pOC6-MMA)** are observed, while λ_{max} values in polymers were not shifted during the photoisomerization. All these results indicate that no aggregation is generated in films because of the low level of azobenzenes. It is worth noting that **p(mMeOC6-MMA)** is also characterized by the relatively large absorbance of the $\Phi-\Phi^*$ band in comparison to that of the $\pi-\pi^*$ band of the molecule and the large energy gap of the $\pi-\pi^*$ and $n-\pi^*$ bands. On the other hand, close-lying of the $\pi-\pi^*$ and $n-\pi^*$ bands is observed in the case of **p(pOC6-MMA)**, where the $n-\pi^*$ band is partly buried.

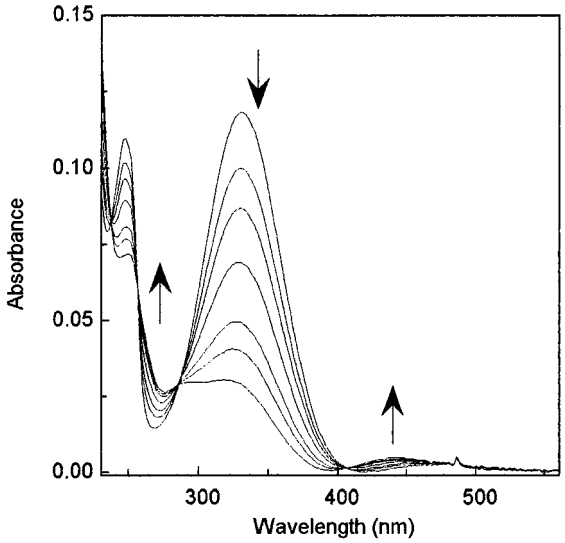

Figure 2. Spectral changes during *E*-to-*Z* photoisomerization induced by 365 nm UV light for a **p(mMeOC6-MMA)** thin film at room temperature. Arrows indicate the directional changes of the spectra.

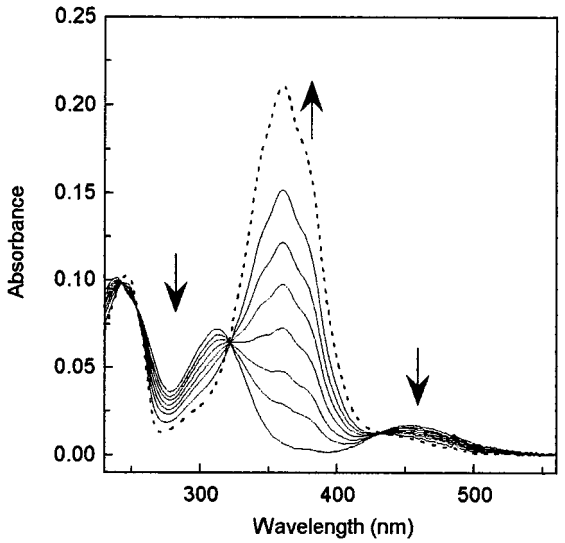

Figure 3. Spectral changes during *Z*-to-*E* photoisomerization induced by 436 nm visible light for a **p(pOC6-MMA)** thin film at room temperature. Arrows indicate the directional changes of the spectra, and the spectrum drawn with a dotted line is that of the virgin film.

Table 2. λ_{max} and *Z*-Fraction *Y* at 365 and 436 nm Light Photostationary States

		in THF			in spin-coated film		
polymer	ϵ_Z/ϵ_E[a]	λ_{max}	Y_{365}	Y_{436}	λ_{max}	Y_{365}	Y_{436}
p(mMeOC6-MMA)	0.082	330	0.92	0.13	330	0.84	0.16
p(pOC6-MMA)	0.010	360	0.99	0.33	360	0.98	0.28

[a] At λ_{max}.

When the ratio of the molar absorption coefficients of the *Z*-isomer (ϵ_Z) and the *E*-isomer (ϵ_E) at a specific wavelength is known, we can calculate *Z*-fractions (Y) during isomerization through the following relation:

$$Y = \frac{[Z]_t}{[E]_0} = \frac{1 - A_t/A_0}{1 - \epsilon_Z/\epsilon_E} \quad (1)$$

Here, the subscripts 0 and t indicate the initial state and reaction at t seconds, respectively. A is the absorbance at which the ratio of ϵ is calculated. We performed the calculation of ϵ_Z/ϵ_E for **p(mMeOC6-MMA)** and **p(pOC6-MMA)** by HPLC, using the low-molecular-weight azobenzenes **mMeOC6Az** and **pOC6Az** and found the value at λ_{max} to be 0.082 and 0.010, respectively. The Y values at the 365 and 436 nm light photostationary states were summarized in Table 2. It is to be noticed that **p(pOC6-MMA)** has a relatively large Y (ca. 0.28) at the 436 nm light photostationary state, different from the cases of other azo-containing polymers, which generally have values of <0.20.

In reversible *E*/*Z* isomerization, the reaction rate is expressed as

$$\frac{d[E]}{dt} = -1000 I_0(\epsilon'_E \phi'_E [E] - \epsilon'_Z \phi'_Z [Z]) \frac{1 - 10^{-A'}}{A'} \quad (2)$$

where $[E]$ (mol dm^{-1}) is the concentration of *E*-isomer, t (s) is the reaction time, ϕ'_E and ϕ'_Z are the partial quantum yields of *E*- and *Z*-isomers at the excitation wavelength, respectively, and A' is the absorbance at the excitation wavelength. The value ϵ' is the molar extinction coefficient at the excitation wavelength. We use the transformation of eq 2 with the introduction of A at λ_{max} into

$$\ln \frac{A_\infty - A_t}{A_\infty - A_0} = -k \int_0^t \frac{1 - 10^{-A'}}{A'} dt \quad (3)$$

to plot the photoisomerization reactions.[7] The slope k ($=1000 I_0[\epsilon'_E \phi'_E + \epsilon'_Z \phi'_Z]$) of this first-order relation is the apparent rate constant, and the integral part, $F(t) = (1 - 10^{-A'})/A'$, is the kinetic factor, related to the absorbed amount of light. The quantum yields can be calculated from the composition at the photostationary state. However, due to the difficulty in determining ϵ_Z', especially in films, and in measuring I_0 accurately enough, we have not attempted to estimate them. Figure 4 shows the plot according to eq 3 for the copolymers exposed to 365 nm light in THF and in film. Whereas the photoisomerization in solution obeyed strictly the simple first-order kinetics, the photoreaction in film exhibited a deviation from first-order kinetics.

The deviation for **p(pOC6-MMA)** (Figure 4b) is more pronounced than that of **p(mMeOC6-MMA)** (Figure 4a). The deviation suggests a combination of fast and slow processes. The fraction of the two processes can be estimated from

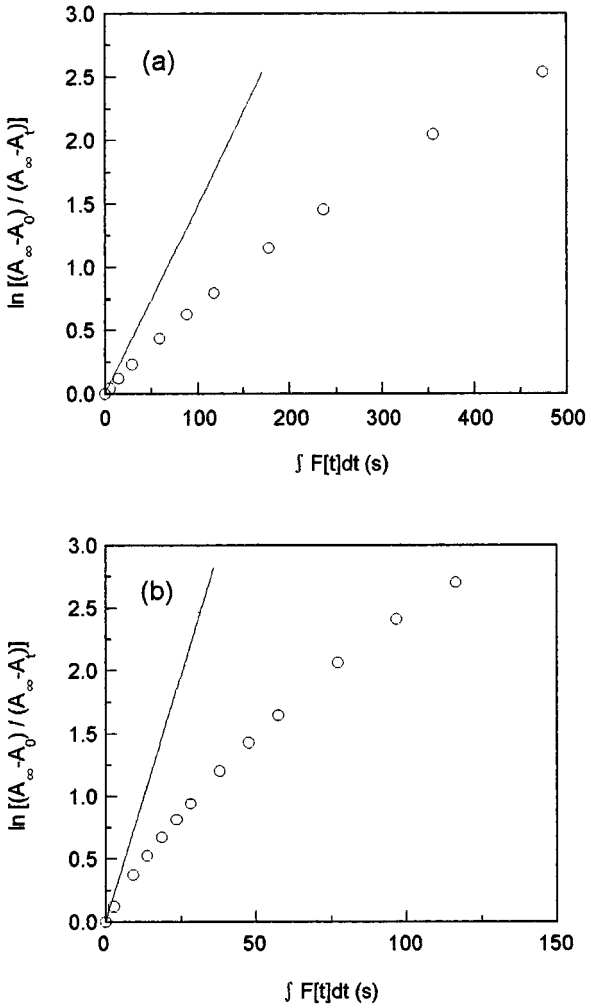

Figure 4. Photoisomerization kinetics induced by 365 nm UV light for (a) **p(mMeOC6-MMA)** and (b) **p(pOC6-MMA)** in THF solutions (solid line) and thin films (circle), performed at room temperature.

$$\frac{A_\infty - A_t}{A_\infty - A_0} = \alpha \exp[-k_f \int_0^t F(t)\, dt] + (1 - \alpha) \exp[-k_s \int_0^t F(t)\, dt] \quad (4)$$

where k_f and k_s are the rate constants for the fast and slow reactions, respectively, and α is interpreted as the fraction of fast photoisomerization to total conversion in the system. The results, also in comparison to those for the low-mass azobenzenes dispersed in PMMA, are summarized in Table 3. The fast isomerization process of the polymers possesses reaction rates close to those in THF. Since the solution photochemistry of low-mass azobenzenes was performed in hexane solutions, the rates were somewhat higher than the corresponding fast rates in PMMA dispersed systems, owing to the polarity of the PMMA matrixes. The polarity effect was confirmed also by the fact that λ_{max} in hexane shows a slight hypsochromic shift.

The fraction of the fast reaction is larger in the cases of systems with 4,4′-disubstituted azobenzenes appearing in the markedly curved first-order plots, as seen for example in Figure 4b. The most important finding here is that the azobenzenes with 3,3′-disubstitution have a larger fraction of the slow reaction $1 - \alpha$ than those with 4,4′-disubstitution. In the work of Robertson et al.,

Table 3. Kinetic Properties of *E*-to-*Z* Photoisomerization at Room Temperature (ca. 20 °C)

			in film			
run	polymer	in THF k^c (s^{-1})	α	$k_f{}^c$ (s^{-1})	1 − α	$k_s{}^c$ (s^{-1})
1	**p(mMeOC6-MMA)**	1.5×10^{-2}	0.35	1.4×10^{-2}	0.65	4.5×10^{-3}
2	**p(pOC6-MMA)**	8.0×10^{-2}	0.45	7.2×10^{-2}	0.55	1.9×10^{-2}
3[b]	**mMeOC6Az**	1.1×10^{-2} [a]	0.54	5.1×10^{-3}	0.46	2.4×10^{-3}
4[b]	**pOC6Az**	6.8×10^{-2} [a]	0.87	2.6×10^{-2}	0.13	6.6×10^{-3}

[a] In hexane solution. [b] PMMA dispersed system. [c] The intensity was roughly constant for all irradiations.

who dealt with polystyrenes incorporating *p*-aminoazobenzene at different specific sites, the fractions of fast processes were also found to be >0.5 with the exception of a chain-centered system (main chain azo-polymer).[3] The annealing history has only a small effect on the fraction of the fast and slow rate processes. They found α to be 0.5 for the side-chain polymer systems and around 0.9 for low-mass azo/PMMA dispersed systems. Notice that these values are in agreement with those of **p(pOC6-MMA)** (run 2) and **pOC6Az**/PMMA (run 4), respectively.

Despite the fact that the photoisomerization mechanisms of azobenzene on $\pi-\pi^*$ excitation are not totally understood, the inversion mechanism is taken as an assumption in the framework of probing the free volume distribution of polymers.[4−6] Nevertheless, the existence of a rotation mechanism is also accepted because of the supporting evidence in the literature mentioned above.

The sweep volume of 3,3′-disubstituted azobenzenes must be smaller than that of 4,4′-disubstituted analogues. The stable *E*- and *Z*-isomers of 3,3′- and 4,4′-disubstituted azobenzene were estimated from semiempirical MOPAC calculation using model compounds as shown in Figure 5.[19] The *Z*-isomers of the model compounds are viewed also from the side-view of one of the planar benzene rings, so that one can estimate the difference in sweep volume during isomerization at a glance. The 4,4′-disubstituted azobenzene needs at least twice as much volume as that needed by the 3,3′-disubstituted azobenzene to isomerize. This suggests that the photoisomerization in polymer systems for 3,3′-disubstituted azobenzene must be less hindered.

Therefore, we believe that two mechanisms could take place here. The emergence of fast and slow processes should reflect both the distribution of free volume and the role of two isomerization mechanisms occurring throughout the reaction. The rotation mechanism needs a larger sweep volume than the inversion does. Since the sweep volume of **p(mMeOC6-MMA)** is smaller, it should be able to undergo rotation in a larger portion than **p(pOC6-MMA)**. Notice that the difference in the fast and slow reaction rates for 3,3′-disubstituted azobenzene is smaller than that for the 4,4′-disubstituted one, suggesting a rather moderate matrix effect on isomerization for the former. Comparing **p(pOC6-MMA)** (run 2) to **pOC6Az** (run 4) or **p(mMeOC6-MMA)** (run 1) to **mMeOC6Az** (run 3), we find that when the azobenzenes are covalently tethered to the polymer backbones as side chains, α decreases. This may be due to the decrease in mobility of the chromophores and the changes of the properties of the polymer matrixes, since the T_g values of azo-bound polymers are lower than those for PMMA (114 °C), which may effect the distribution of free volume.

The kinetics of *Z*-to-*E* photoisomerization was also analyzed by means of first-order plots (Figure 6). In this case, films of the copolymers were first irradiated with

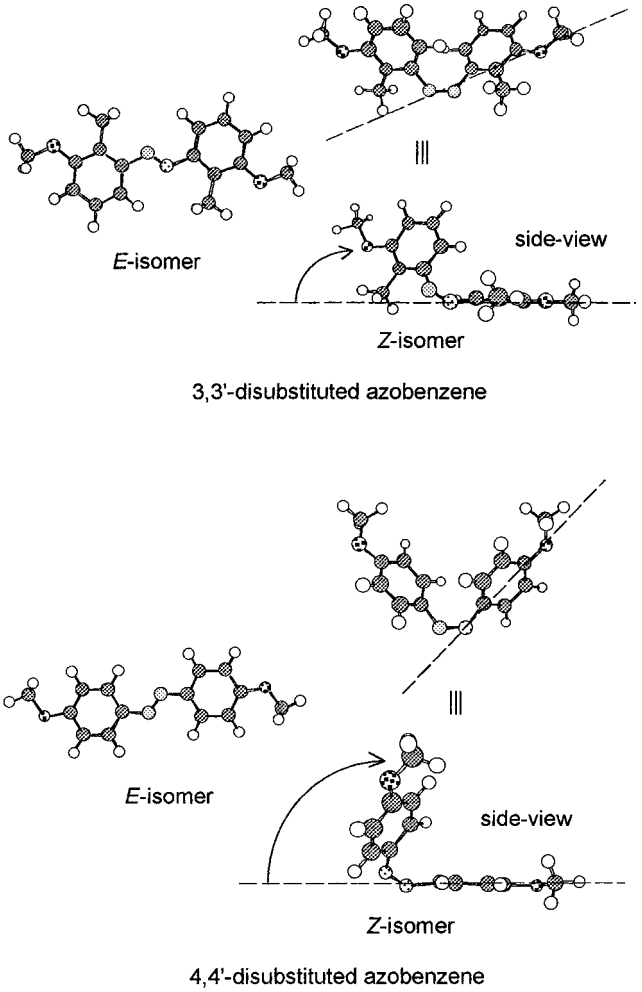

Figure 5. Molecular conformation of *E*- and *Z*-isomers of a 3,3′-substituted azobenzene and a 4,4′-disubstituted azobenzene estimated from semiempirical molecular orbital calculation. The arrows illustrate the apparent change of sweep volume between the two geometrical isomers.

365 nm light at room temperature before irradiation with 436 nm light. Unlike the $\pi-\pi^*$ excitation at 365 nm, the $n-\pi^*$ excitation at 436 nm showed reaction rates approximately the same as that in THF solution. Low-mass azobenzenes dispersed in PMMA also satisfied the first-order rate relation, independent of the positional isomerism of the azobenzenes. In this context, only one mechanism took place, that is the isomerization via inversion route, where the *Z*-to-*E* transformation occurs in a rather two-dimensional way with a relatively small sweep volume within the local free volume of the polymers.

Thermal Isomerization. Thermal *Z*-to-*E* relaxation is followed by tracing the increase of the absorbance at λ_{max} of films primarily exposed to 365 nm light to give photostationary states. The kinetics of the thermal relaxation can be expressed by the following relation:

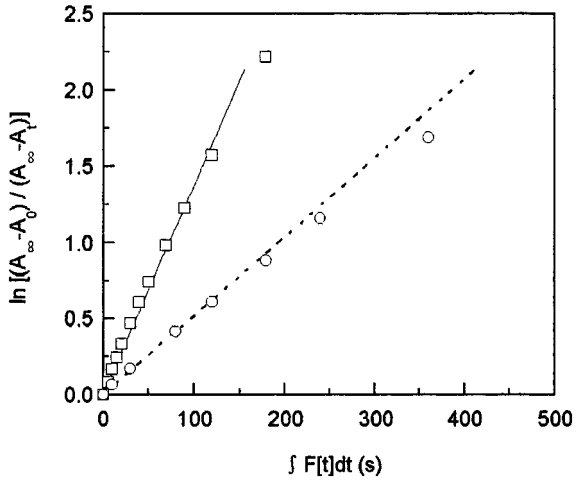

Figure 6. Photoisomerization kinetics induced by 436 nm visible light at room temperature for **p(mMeOC6-MMA)** in THF solution (dotted line) and a thin film (circles) and for **p-(pOC6-MMA)** in THF solution (solid line) and a thin film (squares).

$$\ln \frac{A_\infty - A_0}{A_\infty - A_t} = k_t t \qquad (5)$$

A_0, A_t, and A represent the absorbances at the initial state (a photostationary state after 365 nm light irradiation), at time t, and at an indefinite time to give E-isomers thoroughly, respectively, whereas k_t and t are the rate constant and the reaction time. The thermal relaxation was carried out at several temperatures in a glassy state. From Figure 7, it is obvious that a deviation from eq 5 is observed, suggesting a strong effect of polymer matrixes on the thermal isomerization. Needless to say, in THF solution the reaction shows first-order rates, from which we estimate the Arrhenius parameters.

In a similar way to photoisomerization through $\pi-\pi^*$ excitation, thermal isomerization in a glassy polymer could be resolved as the sum of two simultaneous first-order reactions. In this case the kinetics are described as

$$\frac{A_\infty - A_t}{A_\infty - A_0} = \alpha' \exp(k_f' t) + (1 - \alpha') \exp(k_s' t) \qquad (6)$$

Here α' is interpreted as the fraction of Z-isomer to the total conversion at $t = 0$ which undergoes fast reaction with a rate constant k_f'. Fitting the data to this equation enables a separate calculation of Arrhenius parameters for the fast and slow reactions. From the slopes of Arrhenius plots and the Eyring equation, the apparent activation energies E_a, the frequency factor A, the enthalpy ΔH, and the entropy ΔS are derived. The results are summarized in Table 4. The Z-isomers for **p(mMeOC6-MMA)** are thermally more stable than **p-(pOC6-MMA)**. The half-life times at 25 °C in THF were extrapolated to be 169.6 and 7.3 h, respectively.

It has been pointed out from the work on 4-aminoazobenzene derivatives tethered to the backbone of several methacrylates that the thermal conditions for the E-to-Z photoisomerization would affect significantly α' at the Z-to-E reaction temperature and that this α' increases with reaction temperature under T_g.[10] We investigated thermal Z-to-E relaxation at the glass state within the temperature range of only 15 °C (see Figure 7) and found a very slight increase of α' with temperature, average values being 0.19 ± 0.04 for **p(mOC6-MMA)** and 0.42 ± 0.07 for **p(pOC6-MMA)**. The result for **p(pOC6-MMA)** (at $T - T_g = -41$ to -26) was comparative to that of 4-aminoazobenzene in the mentioned literature. As a matter of fact, the electronic absorption spectra suggest that 4-aminoazobenzene and **p(pOC6-MMA)** belong to the same category of azobenzene, that is the "aminoazobenzene type" azobenzene.[24] However, α' for **mMeOC6-MMA** was low, even though the reactions were performed at temperatures much closer to its T_g (at $T - T_g = -23$ to -8).

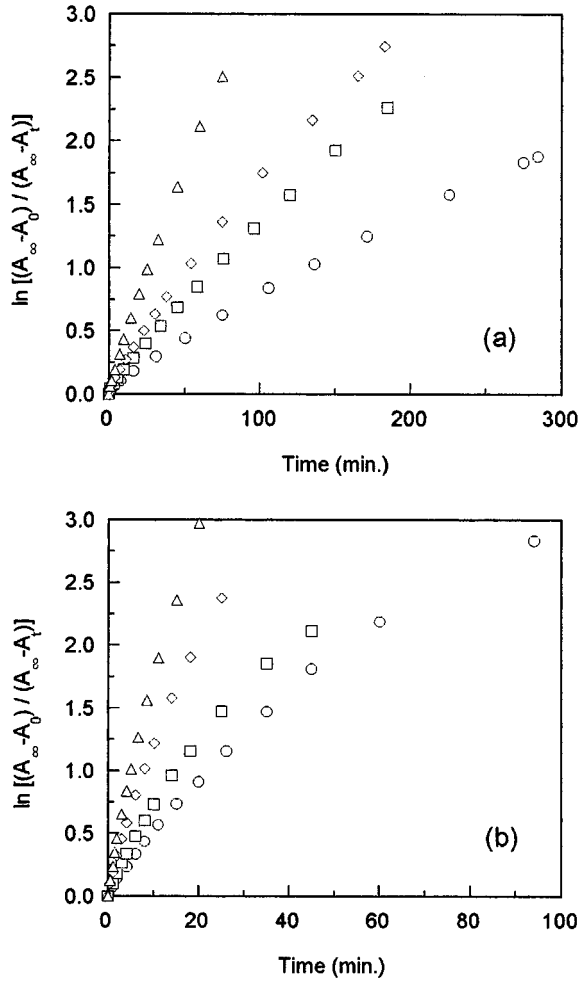

Figure 7. Kinetics of thermal Z-to-E relaxation of (a) **p-(mMeOC6-MMA)** thin films at 70 °C (circles), 75 °C (squares), 78 °C (diamonds), and 85 °C (triangles), and (b) **p(pOC6-MMA)** thin films at 55 °C (circles), 60 °C (squares), 65 °C (diamonds), and 70 °C (triangles).

Following Eisenbach,[9,10] this fast relaxation indicates the translational relaxation of segments of the copolymers incorporating azobenzenes. For **p(mMeOC6-MMA)**, the slow process was dominant, suggesting that this polymer segment relaxes through a local rotational relaxation process on average, likely due to less restriction, reflecting its small sweep volume as discussed above. This is also supported by the ΔS of the process (-10.5 J K^{-1} mol^{-1}) being less negative, indicating a rather favored transition state during relaxation. The large negative value of ΔS (-89.0 J K^{-1} mol^{-1}) for the small portion ($\alpha' = 0.19$) of the fast process in this case is assumed to reflect the steric hindrance as the result of translational relaxation which then involves the rotation of the N−C bond to reach the stable E-form.

Table 4. Arrhenius Parameters of the Thermal *Z*-to-*E* Relaxation of the Polymers in Glassy States

	E_a (kJ mol^{-1})			ln A			ΔS (J K^{-1} mol^{-1})		
		film[a]			film[a]			film[a]	
polymer	in THF	f	s	in THF	f	s	in THF	f	s
p(mMeOC6-MMA)	96.0	78.0	110	25.1	19.9	29.4	−45.5	−89.0	−10.5
p(pOC6-MMA)	83.9	90.5	98.1	24.1	26.8	28.2	−53.8	−31.5	−20.2

[a] f, fast reaction; s, slow reaction.

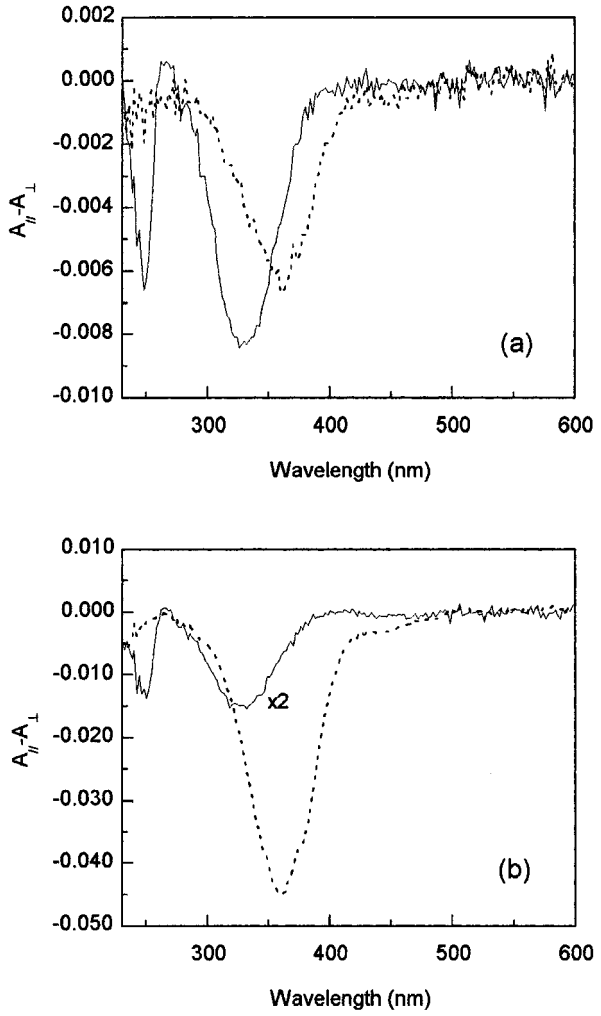

Figure 8. Dichroic spectra ($A_{||}-A_{\perp}$) of thin films of **p(mMeOC6-MMA)** (solid line) and **p(pOC6-MMA)** (dotted line) induced by linearly polarized (a) 365 nm and (b) 436 nm light at photostationary states.

Photoinduced Dichroism. Irradiation with linearly polarized light induced dichroism for thin films of the copolymer. The dichroism is expressed as the order parameter S, defined as

$$S = \frac{A_{||} - A_{\perp}}{A_{||} + 2A_{\perp}} \tag{7}$$

where $A_{\perp}$ and $A_{||}$ are the absorbances of the probe light perpendicular to and parallel to the electric vector of actinic polarized light. The differential spectra ($A_{||} - A_{\perp}$) at photostationary states are shown in Figure 8. Interestingly, in **p(mMeOC6-MMA)** films, we can observe dichroism at the $\Phi - \Phi^*$ band centered at 246 nm, whereas **p(pOC6-MMA)** or other *para*-substituted azobenzene polymers give rise to no dichroism at their $\Phi - \Phi^*$ bands.[23,25] This is probably due to the predominant contribution of the transition moment of the isolated phenyl rings of the 3,3′-disubstituted azobenzene tethered to **p(mMeOC6-MMA)** backbones, which lies parallel to the longitudinal molecular axis of the photooriented chromophore. Figure 9 shows the S of the polymer thin films, being monitored at λ_{max} of the $\pi-\pi^*$ band, as a function of exposure energy of 365 and 436 nm linearly polarized light. Upon irradiation with 365 nm linearly polarized light, the S of **p(pOC6-MMA)** exhibited a maximum value at an exposure energy of approximately 100 mJ cm^{-2}, whereas **p(mMeOC6-MMA)** displays a very weak maximum at a 300 mJ cm^{-2} exposure dose. Prolonged exposure saturated the S values. On the other hand, irradiation with 436 nm polarized light induced a monotonic increase of S for both copolymers.

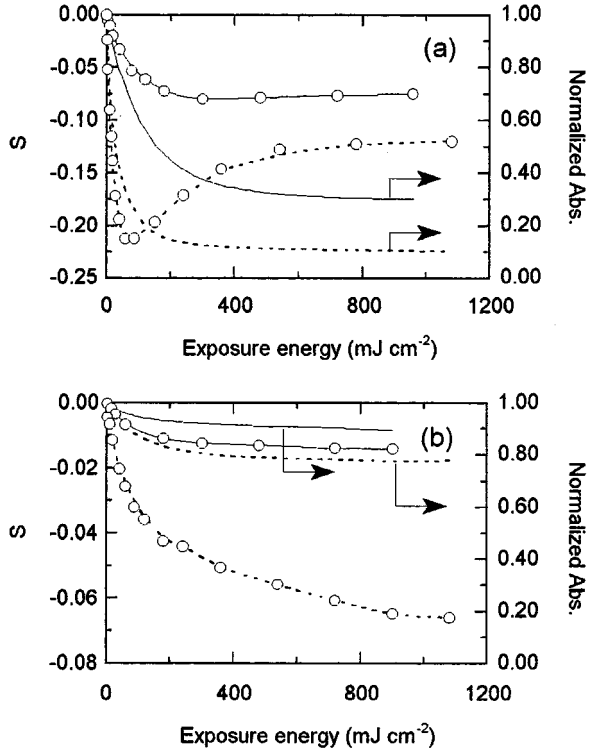

Figure 9. Order parameters of thin films of **p(mMeOC6-MMA)** (solid line) and **p(pOC6-MMA)** (dotted line) calculated from the dichroic spectra after irradiation with linearly polarized (a) 365 nm and (b) 436 nm light. Normalized absorbances are calculated from $(A_{||} + 2A_{\perp})/3A_0$.

The results shown in Figure 9 are explained by the involvement of two photochemical processes, that is axially selective photoisomerization (photoselection), significantly observed at the early stage of 365 nm polarized light irradiation characterized by the emergence of the S maximum, and the alteration of the molecular axis referred to as photoreorientation, which is clearly indicated by the increase of S after the photostationary state.[26] No appearance of a distinct maximum of S for **p(mMeOC6-MMA)** during 365 nm

light irradiation may arise partially from the observation that the level of *E*-to-*Z* conversion is somewhat lower for **p(mMeOC6-MMA)** than that for **p(pOC6-MMA)**, as seen in Table 2. Furthermore, the *Z*-isomer of **mMeOC6-MMA** at a photostationary state possesses a significant absorbance at λ_{max}, at which the *S* is monitored (Figure 2). But these interpretations are not sufficient, since the differences in the contents and in the absorbances of the *Z*-isomer are not so outstanding. The other factor to reduce the maximum *S* value may stem from the fact that the *Z*-isomer of a 3,3′-azobenzene has three conformers, including not only the most stable rodlike one, as illustrated in Figure 5, but also semilinear and bent ones, as discussed in our previous paper.[19] These conformers possess their own different level and direction of transition moments and may be interchangeable after the photoisomerization even though in the polymer matrix, since the rotation around the C−N bond linking phenyl rings and the azo unit requires a relatively small sweep volume. The mixing of the conformers results in the reduction of *S* values more or less.

The saturated *S* value of **p(mMeOC6-MMA)** (−0.014) is anomalously small upon irradiation with polarized 436 nm light when compared to those of the other azobenzene polymers including **p(pOC6-MMA)** ($S = -0.066$). This situation comes from the photoisomerization mechanism as discussed above. *Z*-to-*E* photoisomerization achieved by blue light irradiation takes place through inversion around the azo unit with a small sweep volume, leading to only a moderate deformation of polymer chains surrounding the chromophores. As a result, the *E*/*Z* photoisomerization runs idle without the rearrangement of polymer chains which is suitable for the photoreorientation of the chromopores.

Photoalignment of a Nematic Liquid Crystal. Since the copolymers display dichroism by irradiation with linearly polarized light, their ability as LC photoalignment layers can be anticipated.[17] Hybrid LC cells modified with as-cast films of **p(pOC6-MMA)** and **p(mMeOC6-MMA)** induced a random planar texture of a nematic LC, EXP-CIL. Exposing the cells to linearly polarized 365 nm light gave rise to uniaxially homogeneous alignment for both polymers, which was monitored by measuring the transmittance of the light intensity of a polarized He−Ne laser beam passed through the LC cell and a cross polarizer, respectively, as a function of the rotational angle of the cell around the experimental optical axis, as shown for example in Figure 10. It is surprising to see that despite a very low loading of the chromophores these polymers exhibit the photocontrollability of LC alignment. This makes a contrast to our previous report.[26] Whereas a homopolymer of [2-(4-phenylazophenyl)oxy]ethyl methacrylate gives rise to homogeneous LC alignment with excellent optical quality, no photoalignment of LC was induced by MMA copolymers with 10% loading of the azobenzene monomer. It is very likely that azobenzene moieties of the present copolymers tend to be exposed to an outmost surface of polymer films owing to hydrophobic hexyloxy residues, leading to enhancing a local concentration of the photoreactive units.

An exposure energy as small as 10 mJ cm^{-2}, giving approximately 10% and 35% *E*-to-*Z* conversion for **p(mMeOC6-MMA)** and **p(pOC6-MMA)**, respectively, is enough to change the random alignment to homogeneous alignment. Further irradiation with polarized UV

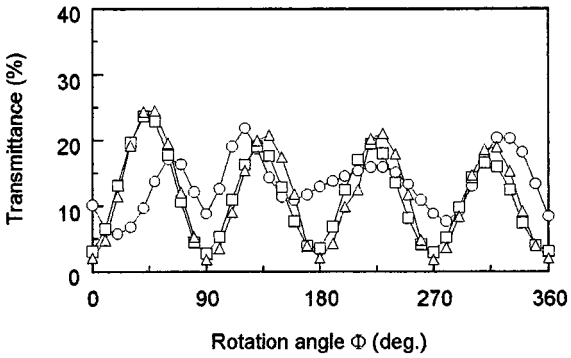

Figure 10. Photoinduced optical axes probed by the angular dependence of the transmitted light intensity of a He−Ne laser beam passed through a hybrid LC cell fabricated by sandwiching a lecithin-treated plate and a glass plate spin-coated with a **p(mMeOC6-MMA)** film, upon exposure to linearly polarized 365 nm light of 0 mJ cm^{-2} (circles), 10 mJ cm^{-2} (squares), and 20 mJ cm^{-2} (triangles).

light did not change the transmittance or the physical appearance of the cell as observed under an optical polarized microscope. On the basis of the results shown in Figure 9, the major contribution to achieve the LC photoalignment is not the photoreorientation but the axis-selective photoisomerization, which consumes azobenzene residues with a molecular direction parallel to the electric vector of the light. As a result, the remaining azobenzenes with a molecular axis perpendicular to the electric vector determine the LC alignment. A similar mechanism of LC photoalignment has been mentioned for polymers with cinnamate side chains.[27] Essentially, there was no difference in exposure energy needed to generate homogeneous LC alignment between the two polymers using polarized 365 nm light.

Irradiation with polarized visible light at 436 nm also resulted in alignment modification of nematic EXP-CIL from random planar to homogeneous alignment. However, in this case, we found that a **p(pOC6-MMA)** film needs about 100 mJ cm^{-2} to be homogeneously photoaligned whereas **p(mMeOC6-MMA)** consumes a dose of 300 mJ cm^{-2}. The dependence of minimum exposure doses required for LC photoalignment on excitation wavelength is definite if we take into account that the azobenzenes can undergo a rotation mechanism upon 365 nm light exposure and an inversion mechanism upon 436 nm light exposure. It is assumed that *E*-to-*Z* photoisomerization, accompanied by a larger sweep volume due to the existence of a rotation mechanism, provides more effective forces to result in the rearrangement of polymer networks when compared with the *Z*-to-*E* photoisomerization, which proceeds only through the inversion mechanism requiring a smaller sweep volume. The fact that **p(mMeOC6-MMA)** needs more exposure energies of polarized visible light to orient as a LC can be attributed to the difference in sweep volumes during the inversion process, as discussed in the following photoreorientation results.

The optical axis of homogeneously aligned LC cells for both polymers lay perpendicular to the direction of the polarized light, as determined by probing absorbances at 633 nm of a doped dichroic aminoanthraquinone dye (LCD118; Merck), which orients parallel to the orientation direction of the LC, with respect to the azimuthal rotational angle of the cells. Additionally, the surface energies of the photoirradiated polymer layers of the two polymers seemed to be less important here,

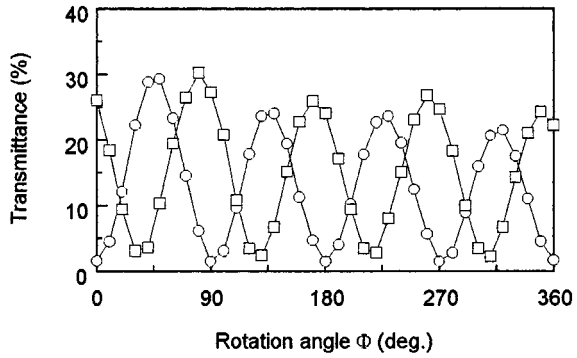

Figure 11. Photoreorientation of LC alignment before (circles) and after (squares) switching the electric vector of linearly polarized 365 nm light at 45° with respect to that of the first polarized light at an exposed energy of 300 mJ cm^{-2} for cells modified with **p(mMeOC6-MMA)**.

Table 5. Contact Angle (deg) of the Polymer Films Measured at 22 °C

		photostationary states	
polymer	virgin film	436 nm light	365 nm light
p(mMeOC6-MMA)	79	78	77
p(pOC6-MMA)	80	78	76

since they appeared to be quite the same (Table 5). This fact supports the idea that the LC photoalignment is performed as a result of intermolecular interactions between surface azobenzenes and LC molecules, as discussed in our previous works.[1]

Photoreorientation of LCs. Since the alignment direction of a LC is superimposed on the direction of perpendicularly oriented azobenzene residues, the photoinduced reorientation of uniaxially photoaligned azobenzenes can be monitored by following the modification of an LC director. When the electric vector of the polarized light is switched 45° with respect to that of the first exposure light, the optical axis of the LC was altered, as shown in Figure 11. The relation between the reorientational optical axis and exposed doses of 365 and 436 nm light, respectively, is shown in Figure 12. The results are summarized as follows. First, large exposure doses are necessary for **p(mMeOC6-MMA)** upon irradiation with both of 365 and 436 nm light. In particular, the exposure doses of visible light leading to the completion of the reorientation for a **p(mMeOC6-MMA)** film are 5.0 J cm^{-2} or more and approximately 10 times larger than that for a **p(pOC6-MMA)** film. Second, the photoreorientation proceeds faster by $\pi-\pi^*$ excitation with 365 nm light for both copolymers when compared with $n-\pi^*$ excitation with 436 nm light. Third, the exposure doses required for the photoreorientation are one order of magnitude greater than those for gaining homogeneous alignment from a random texture; an exposure dose of 10 mJ/cm^2 at the first irradiation with linearly polarized 365 nm light is enough to bring about homogeneous alignment, as stated above.

In the photoreorientation, the azobenzene triggers tethered to polymer backbones are assumed to experience two cooperative rearrangements. First, the $E-Z-E$ transformation takes place until the coincidence of the electric vector of actinic light with the transition moments of azobenzenes is minimized, leading to perpendicular orientation. Second, the rearrangement of segmental chains of the polymers is induced in order to match the new arrangement of the azobenzenes. The

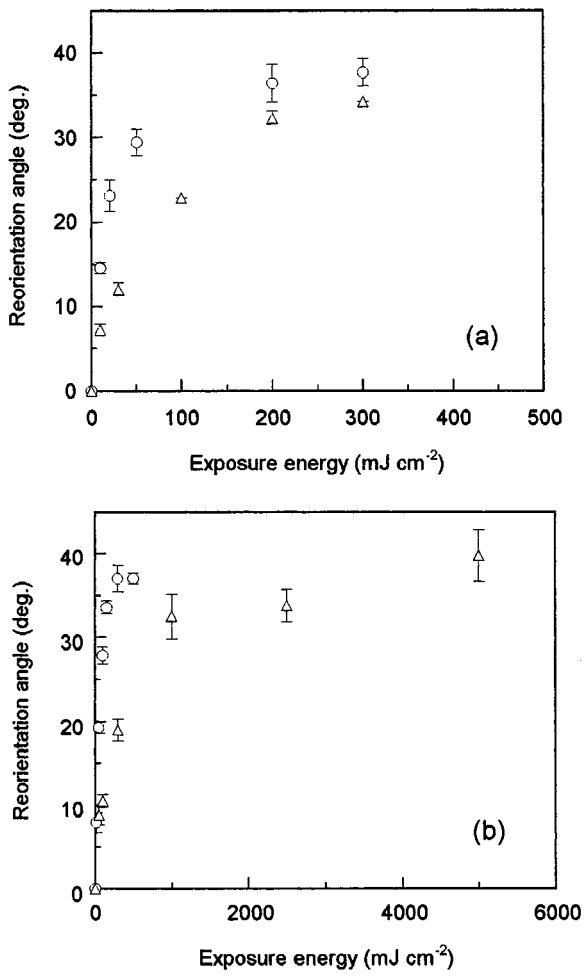

Figure 12. Changes of rotational angles of an optical axis of an LC cell fabricated with **p(mMeOC6-MMA)** (triangles) and **p(pOC6-MMA)** (circles) films with respect to the initial orientational direction, as a function of exposure doses of (a) 365 nm and (b) 436 nm light. The direction of polarized light was switched 45° from that of the first polarized light.

latter process plays a critical role in the photoreorientation because modification of the molecular axis requires a large space which is filled with polymer chains. The force triggering these arrangements stems from the changes of molecular shapes caused by photoisomerization, so that the results shown in Figure 12 can be interpreted in terms of the photoisomerization mechanism and the cooperative rearrangement of the polymer network. The reason markedly larger exposure doses of 436 nm light are required for **p(mMeOC6-MMA)** arises from a relatively small sweep volume of the 3,3′-disubstituted azobenzene side chains through the inversion mechanism, as discussed above. It follows that, when compared with **p(pOC6-MMA)**, the azobenzenes of **p(mMeOC6-MMA)** display less sufficient forces to elbow through the crowded polymer chains so that large exposure doses are consumed. This interpretation can also be applied to the understanding of the faster processes through $\pi-\pi^*$ excitation. Finally, the requirement for the photoreorientation induced by polarized 365 nm light as compared with the initial generation of homogeneous alignment is interpreted decisively by the difference in the photoalignment mechanism. As mentioned above, the random-to-homogeneous alignment change is triggered by the axis-selective E-to-Z photoisomerization without a photoinduced reorientational process. On the contrary, the reorientation of the

homogeneous LC alignment has to be caused by the reorientation of azobenzene side chains upon the second polarized light irradiation. This process requires a large sweep volume and subsequently large exposure doses. The difference in the required exposure doses for both copolymers is evidently due to the difference in sweep volume during *E*-to-*Z* photoisomerization, as illustrated in Figure 5. The larger sweep volume in **p(pOC6-MMA)** brings about the rearrangement of polymer chains more sufficiently.

Conclusion

Studies comparing the isomerization behavior of polymethacrylates bearing 3,3′-disubstituted azobenzenes as side chains (**p(mMeOC6-MMA)**) with that of polymethacrylates having 4,4′disubstituted azobenzene side chains (**p(pOC6-MMA)**) provide novel information concerning the isomerization mechanism in polymer solids. The kinetics studies on the *E*-to-*Z* photoisomerization of the copolymers in their glassy state by 365 nm light irradiation revealed that the contribution of the rotation mechanism must be more pronounced for 3,3′-disubstituted azobenzene moieties tethered to polymer backbones when compared with 4,4′-disubstituted ones because of a smaller sweep volume of the former during the isomerization. On the other hand, the *Z*-to-*E* photoisomerization of both copolymers induced by 436 nm light obeyed simple first-order kinetics similar to those for the photoisomerization in solutions due to the inversion mechanisms taking place there, where the sweep volumes were relatively smaller than those required for the rotational isomerization. As for thermal isomerization, *Z*-to-*E* thermal relaxation in the solid state consisted of two fast and slow processes for both copolymers in a conventional manner, while the fractions for both processes were different from each other. The fraction for the fast relaxation exhibiting a smaller energy of activation E_a was much smaller for **p(mMeOC6-MMA)** than for **p(pOC6-MMA)**. Furthermore, the slow relaxation of **p(mMeOC6-MMA)** was characterized crucially by the entropy being less negative, suggesting quite a stable transition state, likely due to less restriction of the surroundings. This situation also reflects the sweep volume of **p(mMeOC6-MMA)** being smaller because of the inversion mechanism in the thermal process.

It was confirmed that the dichroism of azobenzene side chains by illumination with linearly polarized 365 nm light is generated as a result of two processes consisting of axis-selective *E*-to-*Z* photoisomerization and photoreorientation upon prolonged irradiation. The photogeneration of optical anisotropy by polarized light irradiation is also influenced by isomerization mechanisms. The anomalously small order parameter observed for **mMeOC6-MMA** exposed to linearly polarized 436 nm light arises from the inversion mechanism, which leads to such a small sweep volume that the rearrangement of polymer chains required for the reorientation of the molecular axis is hardly caused.

The azimuthal alignment of a nematic LC can be controlled for thin films of both the copolymers by linearly polarized light irradiation even though the level of azobenzene units is low. The photoinduced reorientation of a LC gives novel information concerning the modification of the molecular axis of uniaxially photoaligned azobenzenes. The exposure doses of polarized 436 nm light for the LC reorientation by using **p(mMeOC6-MMA)** were one order of magnitude greater than the moderated exposure doses of polarized 365 nm light for the photoreorientation of LC molecules triggered by both copolymers and of polarized 436 nm light for that by **p(pOC6-MMA)**. This observation stems again from the inversion of the 3,3′-disubstituted azobenzene requiring a small sweep volume.

References and Notes

(1) Ichimura, K. In *Polymers as Electrooptical and Photooptical Active Media*; Shibaev, V. P., Ed.; Springer: Berlin, 1996; Chapter 4, p 138.
(2) Victor, J. G.; Torkelson, M. *Macromolecules* **1987**, *20*, 2241.
(3) Yu, W. C.; Sung, C. S. P.; Robertson, R. E. *Macromolecules* **1988**, *21*, 355.
(4) Mita, I.; Horie, K.; Hirao, K. *Macromolecules* **1989**, *22*, 558.
(5) Naito, T.; Horie, K.; Mita, I. *Macromolecules* **1991**, *24*, 2907.
(6) Naito, T.; Horie, K.; Mita, I. *Polymer* **1993**, *34*, 4140.
(7) Shen, Y. Q.; Rau, H. *Makromol. Chem.* **1991**, *192*, 945.
(8) Paik, C. S.; Morawetz, H. *Macromolecules* **1972**, *5*, 171.
(9) Eisenbach, C. D. *Makromol. Chem.* **1978**, *179*, 2489.
(10) Eisenbach, C. D. *Ber. Bunsen-Ges. Phys. Chem.* **1980**, *84*, 680.
(11) Haitjema, H. J.; von Morgen, G. L.; Yong Tan, Y.; Challa, G. *Macromolecules* **1994**, *27*, 6201.
(12) Rau, H. *J. Photochem.* **1984**, *26*, 221.
(13) Rau, H.; Luddecke, E. J. *J. Am. Chem. Soc.* **1982**, *104*, 1616.
(14) Asano, T.; Okada, T. *J. Org. Chem.* **1984**, *49*, 4387.
(15) Monti, S.; Orlandi, G.; Palmieri, P. *J. Chem. Phys.* **1982**, *71*, 87.
(16) Ichimura, K.; Suzuki, Y.; Seki, T.; Hosoki, A.; Aoki, K. *Langmuir* **1988**, *4*, 1214.
(17) Ichimura, K. *Supramol. Sci.* **1996**, *3*, 67.
(18) Ruslim, C.; Ichimura, K. *Chem. Lett.* **1998**, 789.
(19) Ruslim, C.; Ichimura, K. *J. Mater. Chem.* **1999**, *9*, 673.
(20) Law, K. L.; Loutfy, R. O. *Macromolecules* **1981**, *14*, 587.
(21) Seki, T.; Fukuda, R.; Tamaki, T.; Ichimura, K. *Thin Solid Films* **1994**, *243*, 675.
(22) Buffeteau, T.; Pézolet, M. *Macromolecules* **1998**, *31*, 2631.
(23) Menzel, H.; Rüther, M.; Stumpe, J.; Fischer, T. *Supramol. Sci.* **1998**, *5*, 49.
(24) Rau, H. In *Photochromism: Molecules and Systems*; Dürr, H., Bouas-Laurent, H., Eds.; Elsevier: Amsterdam, 1990; Chapter 4, p 165.
(25) Stumpe, J.; Geue, Th.; Fischer, Th.; Menzel, H. *Thin Solid Films* **1996**, *284*, 606.
(26) Akiyama, H.; Kudo, K.; Ichimura, K. *Macromol. Rapid Commun.* **1995**, *16*, 35.
(27) Ichimura, K.; Akita, Y.; Akiyama, H.; Kudo, K.; Hayashi, Y. *Macromolecules* **1997**, *30*, 903.

MA990102D